NOLTA, IEICE

Paper

Typical patterns of oscillations in three-phase circuit

Takashi Hisakado [1 a)] *and Shota Ukai* [1]

[1] *Department of Electrical Engineering, Kyoto University Nishikyo, Kyoto 615-8510, Japan*

[a)] *hisakado@kuee.kyoto-u.ac.jp*

Abstract: Symmetrical three-phase circuits are fundamental models of power systems. Although the circuits have structural symmetry, asymmetric patterns of oscillations have been observed in real power systems. This paper describes an approach to understanding typical patterns of oscillations in the three-phase circuits using symmetry. In order to figure out oscillation patterns, we introduce a three LC ladder circuit which has a higher symmetry than the three-phase circuit. Using only the symmetries of the three LC ladder circuit, we classify periodic oscillations and construct a lattice of those modes. Further, extending the method to almost periodic oscillations, we decompose and characterize typical almost periodic oscillations by their symmetry. Finally, by observing a global phase space in the three LC ladder circuit, we confirm typical oscillations in the three-phase circuit.

Key Words: three-phase circuit, power system, symmetry, ferroresonance, nonlinear normal mode, intrinsic localized modes

1. Introduction

The wide variety of power systems, such as dispersed power sources and power electronic systems, leads to interest in crucial disturbances in electric power systems. Especially, it is important to understand nonlinear phenomena in power systems, e.g., voltage collapse, ferroresonance, and dynamical behaviors of nonlinear components such as power converters and flexible ac transmission systems (FACTS) devices.

Ferroresonance is a nonlinear oscillatory phenomenon leading to dangerous overvoltages in power equipment and is caused by a nonlinearity of transformers [1–4]. The oscillation was first reported in [5] and has been extensively studied over the past 100 years [1]. The first analytical work of fundamental harmonic, subharmonic and higher harmonic oscillations was done by R. Rudenberg [6] and more exact and detailed work which contains almost periodic oscillations was done by C. Hayashi [7]. Y. Ueda observed chaos in the research of a ferroresonance system in 1961 [8]. Subsequent research from the bifurcation theoretic framework was reported in [3, 9–13]. Another approach to ferroresonance in power systems is oscillation patterns in the structure of three-phase circuits [14–18]. The word "pattern" means types of oscillations based on the structural symmetry of the three-phase circuit [19, 20]. The detailed analyses of each oscillation type are reported for subharmonic oscillations [12, 21, 22], asymmetric oscillations [12, 21, 23, 24], cnoidal waves [25] and intrinsic localized modes (ILMs) [26]. Although the bifurcations of each oscillation are analyzed in detail, systematic approaches to finding out those patterns have not been reported. This paper focuses on figuring out the typical patterns of

[Received: November 10, 2010. Revised: February 1, 2011. Published: July 1, 2011.]
[DOI: 10.1588/nolta.2.320]
Nonlinear Theory and Its Applications, IEICE, vol. 2, no. 3, pp. 320–331

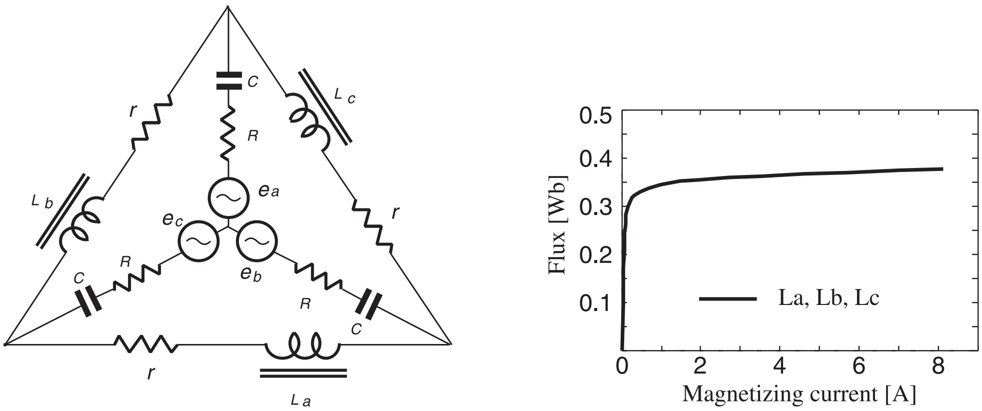

Fig. 1. Three-phase circuit and nonlinear characteristics of fluxes in real experiment.

oscillations in a three-phase circuit only by its symmetry.

In linear systems, the patterns of the oscillations are easily figured out by the concept of normal mode. The extension of the linear normal mode to nonlinear systems is first reported in [27] and subsequent research is reviewed by [28]. Discussions from the symmetry of systems are reported in the researches of FPU lattice [29–31]. Another approach to listing the typical oscillation patterns is reported in [19, 20]. The method works out a catalog of typical forms of behavior using only the symmetries of a system. In this paper, we introduce a three LC ladder circuit which has higher symmetry than the three-phase circuit, and applying the method in [19, 20], we make a list of the oscillation patterns and figure out typical oscillations in three-phase circuits.

In section 2, we review the typical oscillations in a three-phase circuit by experimental results. In section 3, we derive the three LC ladder circuit and show the symmetries of the three LC ladder circuit. In section 4, we classify the periodic oscillations with respect to the symmetries and we extend the method to almost periodic oscillations in section 5.

2. Typical oscillations in three-phase circuit

We review typical oscillations in a fundamental three-phase circuit shown in Fig. 1. The circuit consists of Δ-connected inductors and resistors, and Y-connected capacitors and resistors, and three-phase voltage sources. The three inductors have nonlinear characteristics of fluxes. The characteristics of the nonlinear inductors used in our experiment are also shown in Fig. 1.

The patterns of oscillations generated in three-phase circuits are classified into the following three types [15, 17, 18, 21, 22] based on the number of related inductors:

Type 1: Oscillations mainly excited by any one of the three inductors. The current flows dominantly through only one inductor and the three-phase circuit operates as if it were a single-phase circuit.

Type 2: Oscillations mainly excited by any two of the three inductors. The currents flow dominantly through only two inductors and the three-phase circuit operates as if it were a two-phase circuit.

Type 3: Oscillations excited by all the three inductors. Normal oscillations in three-phase power systems belongs to this type.

Figure 2 shows typical fundamental harmonic oscillations observed by the experiment. The E_a and I_a, I_b, I_c denote the voltage waveform of E_a and the current waveforms of inductors a, b and c, respectively. The left figure shows a fundamental harmonic type 3 oscillation in which the phases of the three inductor currents are three-phase and this oscillation is a normal oscillation forced by three-phase voltage sources. The right figure shows a fundamental harmonic type 1 oscillation. A cnoidal wave shown in Fig. 3 is a strange oscillation [14, 25], but it is a type 3 oscillation in this classification. The waveform of the cnoidal wave shows that the current pulses of every inductor circulate in the Δ connection and the direction of the circulation suddenly changes every about 125 ms.

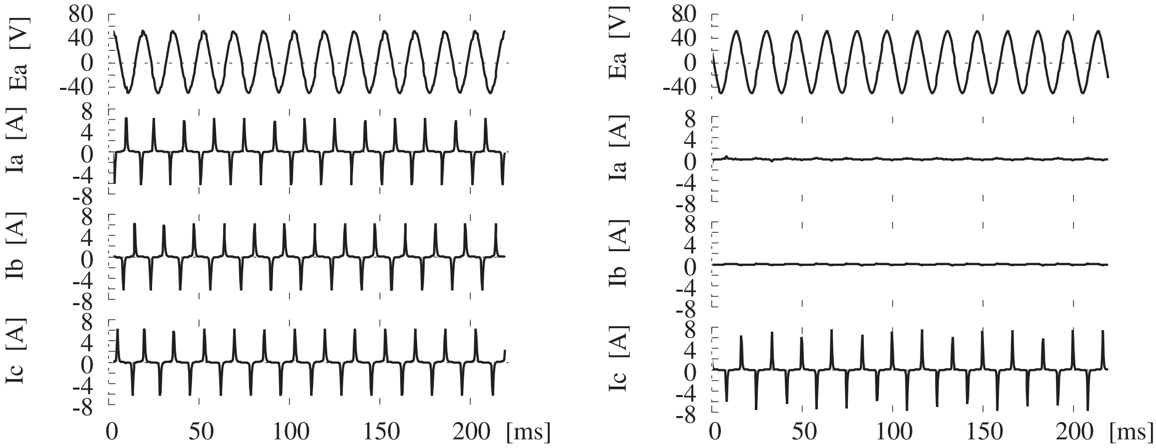

Fig. 2. Typical fundamental harmonic oscillations (real experiment with $R = 2.5\Omega$, $r = 3.1\Omega$ and $1/\omega C = 42.2\Omega$ [24]). The E_a, I_a, I_b, I_c are the voltage waveform of E_a and the current waveforms of inductors a, b and c, respectively. The left figure is type 3 and the right figure is type 1.

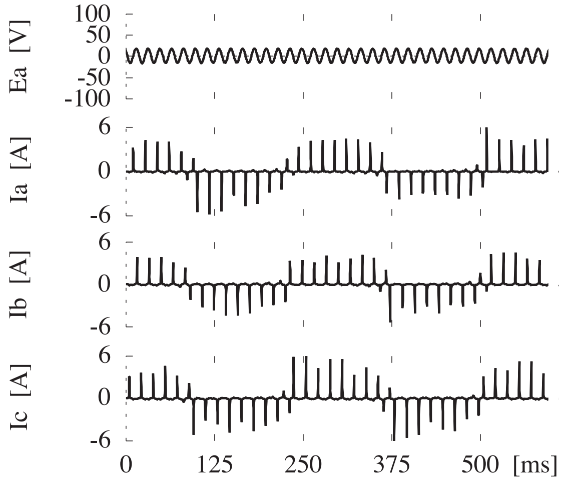

Fig. 3. Cnoidal wave in fundamental harmonic oscillations (real experiment with $R = 2.5\Omega$, $r = 3.1\Omega$ and $1/\omega C = 44.2\Omega$ [25]). The current pulses of every inductor circulate in the Δ connection and the direction of the circulation suddenly changes every about 125 ms.

These patterns are observed also in subharmonic oscillations [12]. Figure 4 shows the two patterns of 1/3-subharmonic oscillations. The left figure is a 1/3-subharmonic type 3 oscillation and the right figure is a 1/3-subharmonic type 1 oscillation. In this case the type 3 oscillation is an almost periodic oscillation. In 1/3-subharmonic oscillation, a type 2 oscillation shown in Fig. 5 is also reported in [23]. These oscillation patterns are observed also for other subharmonic oscillations [22]. The objective of this paper is to give a reason for the generation of these typical oscillations using the symmetry of the circuit.

3. Three LC ladder circuit and its symmetry

3.1 Circuit equation of the three-phase circuit

The normalized equation of the three-phase circuit shown in Fig. 1 is described by

$$\frac{\mathrm{d}}{\mathrm{d}t}\begin{pmatrix} \boldsymbol{\psi}_{\mathrm{abc}} \\ \boldsymbol{u}_{\mathrm{abc}} \end{pmatrix} = \begin{pmatrix} -\boldsymbol{A}_{\mathrm{abc}}\boldsymbol{u}_{\mathrm{abc}} & +\boldsymbol{e}_{\mathrm{abc}} - \boldsymbol{R}_{\mathrm{abc}}\boldsymbol{i}_{\mathrm{abc}} \\ \boldsymbol{A}_{\mathrm{abc}}^{\mathrm{T}}\boldsymbol{i}_{\mathrm{abc}} & \end{pmatrix}. \tag{1}$$

$$\boldsymbol{A}_{\mathrm{abc}} \triangleq \begin{pmatrix} 0 & 1 & -1 \\ -1 & 0 & 1 \\ 1 & -1 & 0 \end{pmatrix},$$

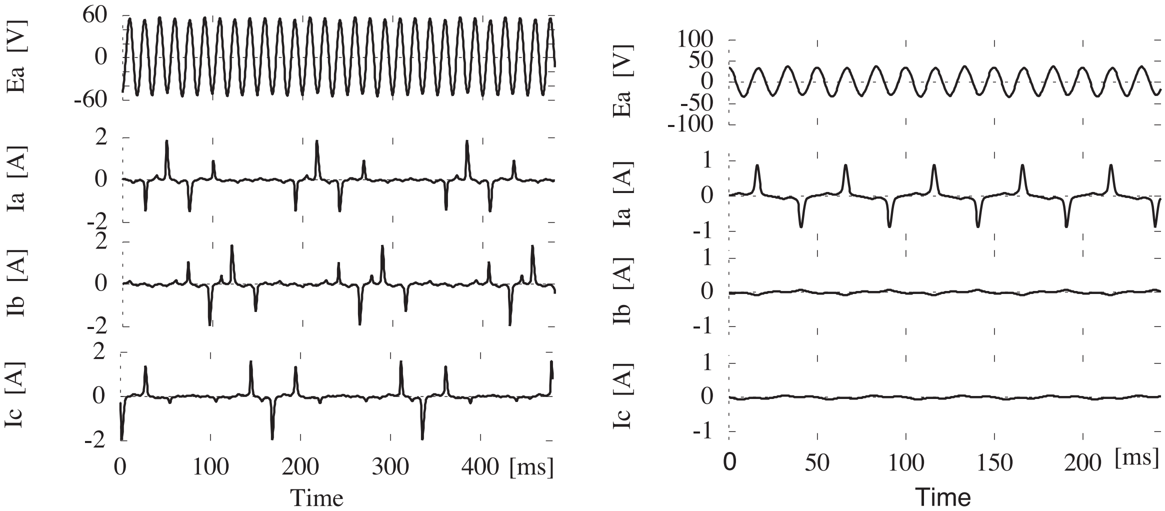

Fig. 4. Typical 1/3-subharmonic oscillations (real experiment with $R = 12.3\Omega$, $r = 3.1\Omega$ and $1/\omega C = 13.6\Omega$ (left figure)/ $1/\omega C = 27.2\Omega$ (right figure) [12]).

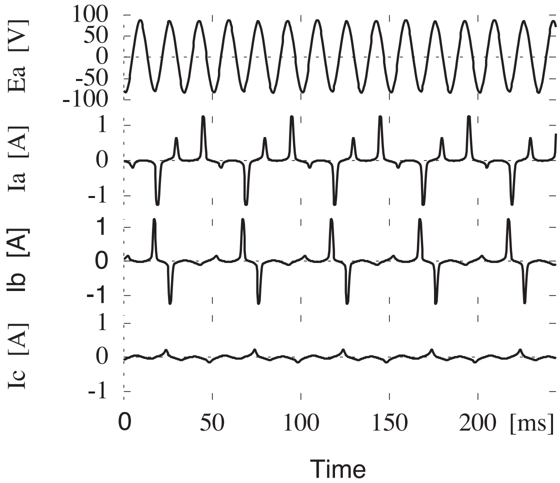

Fig. 5. 1/3-subharmonic type 2 oscillation (real experiment with $R = 12.3\Omega$, $r = 3.1\Omega$ and $1/\omega C = 14.7\Omega$ [23]).

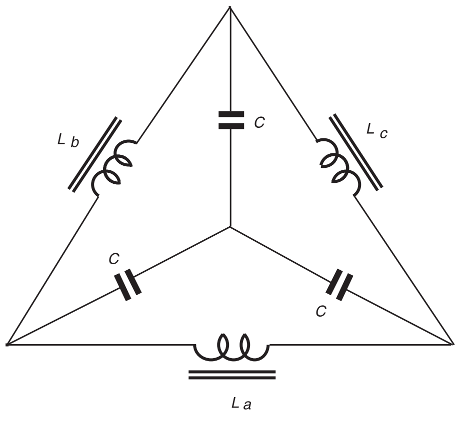

Fig. 6. Three LC ladder circuit.

$$
\begin{array}{lll}
\boldsymbol{\psi}_{\mathrm{abc}} & \triangleq (\psi_{\mathrm{a}}, \psi_{\mathrm{b}}, \psi_{\mathrm{c}})^{\mathrm{T}} & : \text{fluxes of the inductors} \\
\boldsymbol{u}_{\mathrm{abc}} & \triangleq (u_{\mathrm{a}}, u_{\mathrm{b}}, u_{\mathrm{c}})^{\mathrm{T}} & : \text{voltages of the capacitors} \\
\boldsymbol{R}_{\mathrm{abc}} & \triangleq \boldsymbol{A}_{\mathrm{abc}}^{\mathrm{T}} \boldsymbol{A}_{\mathrm{abc}} R + \boldsymbol{I} r & : \text{matrix for resistors} \\
\boldsymbol{i}_{\mathrm{abc}}(\boldsymbol{\psi}_{\mathrm{abc}}) & \triangleq (i(\psi_{\mathrm{a}}), i(\psi_{\mathrm{b}}), i(\psi_{\mathrm{c}}))^{\mathrm{T}} & : \text{currents of the inductors} \\
\boldsymbol{e}_{\mathrm{abc}}(t) & \triangleq E_{\mathrm{abc}}(\sin(\omega_e t), \sin(\omega_e t - \frac{2\pi}{3}), \sin(\omega_e t + \frac{2\pi}{3}))^{\mathrm{T}} & : \text{three-phase voltage source,}
\end{array}
$$

where the $\boldsymbol{I}$ denotes unit matrix and $(*)^{\mathrm{T}}$ denotes transposition. The R, r, ω_e represent normalized circuit parameters which corresponds to Y-connected resistors, Δ-connected resistors, and angular frequency of the voltage sources, respectively. We assume that the characteristics of the flux $i(\psi)$ is represented by a monotone increasing odd function.

3.2 Three LC ladder circuit

In order to find typical patterns in the three-phase circuit, we introduce a higher symmetric circuit. First, the elimination of the three-phase voltage source from the three-phase circuit gives the reflection symmetry. Second, the elimination of resistors gives periodic and almost periodic free oscillations in the circuit. As a result, we obtain a three LC ladder circuit shown in Fig. 6. The equation of the circuit is described by

$$\frac{\mathrm{d}}{\mathrm{d}t}\begin{pmatrix} \boldsymbol{\psi}_{\mathrm{abc}} \\ \boldsymbol{u}_{\mathrm{abc}} \end{pmatrix} = \begin{pmatrix} -\boldsymbol{A}_{\mathrm{abc}}\boldsymbol{u}_{\mathrm{abc}} \\ \boldsymbol{A}_{\mathrm{abc}}^{\mathrm{T}}\boldsymbol{i}_{\mathrm{abc}} \end{pmatrix}. \tag{2}$$

For simplicity, we rewrite Eq. (2) by

$$\frac{\mathrm{d}\boldsymbol{x}_{\mathrm{abc}}}{\mathrm{d}t} = \boldsymbol{f}_{\mathrm{abc}}(\boldsymbol{x}_{\mathrm{abc}}), \qquad \boldsymbol{x}_{\mathrm{abc}} = (\boldsymbol{\psi}_{\mathrm{abc}}^{\mathrm{T}},\ \boldsymbol{u}_{\mathrm{abc}}^{\mathrm{T}})^{\mathrm{T}}. \tag{3}$$

Although Eq. (2) is a conservative system and does not have attractors, its symmetry reveals the typical patterns observed in real experiments. We will discuss the symmetry and oscillation patterns using Eq. (3) in subsequent sections.

3.3 Symmetries of three LC ladder circuit

The Eq. (3) of the LC ladder circuit has the symmetry of the dihedral group $\boldsymbol{D}_6$ because LC ladder circuit has symmetries of cyclic permutation, reflection and inversion based on the odd function. We define generators ρ and σ of $\boldsymbol{D}_6$ by

$$\rho(\psi_a, \psi_b, \psi_c, u_a, u_b, u_c)^{\mathrm{T}} = (\psi_b, \psi_a, \psi_c, -u_b, -u_a, -u_c)^{\mathrm{T}} \tag{4}$$
$$\sigma(\psi_a, \psi_b, \psi_c, u_a, u_b, u_c)^{\mathrm{T}} = (-\psi_a, -\psi_c, -\psi_b, u_a, u_c, u_b)^{\mathrm{T}}. \tag{5}$$

If we let I denote the identity map, and define $\tau \triangleq \sigma\rho$, then $\tau^3 = -I$ and $\tau^6 = I$. If $\rho, \sigma, \cdots$ are elements of $\boldsymbol{D}_6$, let $\langle \rho, \sigma, \cdots \rangle$ denote the subgroup of $\boldsymbol{D}_6$ generated by $\rho, \sigma, \cdots$. Then, representative subgroups of each conjugacy class of subgroups of $\boldsymbol{D}_6$ are

$$\langle -I \rangle = \boldsymbol{Z}_2 \tag{6}$$
$$\langle \rho \rangle = \boldsymbol{Z}_2^{\rho}(\cong \boldsymbol{Z}_2) \tag{7}$$
$$\langle \sigma \rangle = \boldsymbol{Z}_2^{\sigma}(\cong \boldsymbol{Z}_2) \tag{8}$$
$$\langle \tau^2 \rangle = \boldsymbol{Z}_3 \tag{9}$$
$$\langle \rho, -I \rangle = \boldsymbol{D}_2^{\rho}(\cong \boldsymbol{D}_2) \tag{10}$$
$$\langle \tau^2, \rho \rangle = \boldsymbol{D}_3^{\rho}(\cong \boldsymbol{D}_3) \tag{11}$$
$$\langle \tau^2, \sigma \rangle = \boldsymbol{D}_3^{\sigma}(\cong \boldsymbol{D}_3) \tag{12}$$
$$\langle \tau \rangle = \boldsymbol{Z}_6 \tag{13}$$

together with $\boldsymbol{D}_6$ and the trivial subgroup $E = \{I\}$, where $\boldsymbol{Z}_n$ denotes the cyclic group of order n and $\boldsymbol{D}_n$ denotes the dihedral group of order $2n$ [19, 20].

4. Classification of periodic oscillations

4.1 Spatio-temporal symmetry and spatial symmetry

In order to list typical patterns of periodic oscillations, we define the period T oscillation $\boldsymbol{x}_{\mathrm{abc}}(t)$ in the three LC ladder circuit by

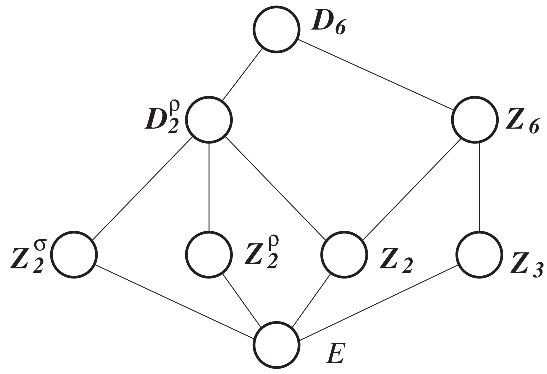

Fig. 7. Lattice of symmetric periodic oscillations.

$$\boldsymbol{x}_{\mathrm{abc}}(t) = \boldsymbol{x}_{\mathrm{abc}}(t+T). \tag{14}$$

We normalize the time t by the period T and consider period 2π oscillation $\hat{\boldsymbol{x}}(\theta) : \mathbb{T}^1 \mapsto \mathbb{R}^6$, where θ is a normalized phase and $\mathbb{T}^1$ denotes 1-torus.

Although the system has many subgroups, the symmetries of the periodic oscillation are limited. Let us consider a subgroup $H \subset \boldsymbol{D}_6$. If a periodic oscillation $\hat{\boldsymbol{x}}(\theta)$ satisfies

$$H = \{\gamma \in \boldsymbol{D}_6 \mid \gamma\{\hat{\boldsymbol{x}}(\theta)\} = \{\hat{\boldsymbol{x}}(\theta)\}\} \tag{15}$$

for all the actions $\gamma \in H$, the periodic oscillation has spatio-temporal symmetry [20]. This relation means that the H-action preserves the trajectory of $\hat{\boldsymbol{x}}(\theta)$ and an action $\gamma \in H$ causes only a shift k:

$$^\forall\theta \in \mathbb{T}^1,\ \gamma\hat{\boldsymbol{x}}(\theta) = \hat{\boldsymbol{x}}(\theta - k). \tag{16}$$

We represent the correspondence between γ and k by a map $k = \Theta(\gamma)$. Then, the kernel of the map Θ is defined by

$$K \triangleq \{\gamma \in H \mid \Theta(\gamma) = 0\}. \tag{17}$$

The kernel K derives a fixed-point subspace

$$\mathrm{Fix}(K) \triangleq \{\hat{\boldsymbol{x}} \in \mathbb{R}^6 \mid \gamma\hat{\boldsymbol{x}} = \hat{\boldsymbol{x}},\ \ ^\forall\gamma \in K\} \subset \mathbb{R}^6. \tag{18}$$

In this sense, the subgroup K represents spatial symmetry of the three LC ladder circuit. For the existence of periodic oscillations, it is necessary that H/K is isomorphic to cyclic group $\boldsymbol{Z}_m$ and that the dimension of $\mathrm{Fix}(K)$ is not less than 2 [20].

Based on the above conditions, we classify the symmetric periodic oscillations with respect to the subgroups H and K. The patterns of oscillations are listed in Table I, where $\eta, \xi, \zeta : \mathbb{T}^1 \mapsto \mathbb{R}^1$ are period 2π functions. Labels M_1, M_2 and M_3 in the table denote typical highly symmetric type 1, type 2 and type 3 periodic oscillations, respectively. Further, Fig. 7 shows the lattice of symmetric periodic oscillations in the three LC ladder circuit with respect to the spatio-temporal symmetry H. The M_1 and M_2 belong to a subgroup $\boldsymbol{D}_2^\rho$ and the M_3 belongs to a subgroup $\boldsymbol{Z}_6$.

4.2 Examples of highly symmetric oscillations

Let us discuss the typical highly symmetric oscillations M_1, M_2, and M_3 shown in Figs. 8, 9, and 10, respectively. The waveforms are calculated by a function $i(\psi) = \psi + 3.8\psi^7$, which is given to approximate the characteristics of fluxes shown in Fig. 1. The M_1 and M_2 are symmetric with respect to the reflection and the inversion. The difference between the M_1 and the M_2 comes from the spatial symmetry K. It is noted that the experimental results in Figs. 2, 4, and 5 show the currents and that the example waveforms Figs. 8, 9, and 10 show the fluxes. From the viewpoint of ILM, the M_1 and M_2 correspond to ST mode and Page mode, respectively [31]. The M_3 is symmetric with respect to $\boldsymbol{Z}_6$ and the shift $k = +\mathrm{k}_3$ and $k = -\mathrm{k}_3$ represent the propagating directions. Thus, the symmetries of the three LC ladder circuit give the patterns of oscillations.

Table I. Pattern of oscillations.

H	K	label	$\boldsymbol{\psi}_{\mathrm{abc}}$			comments
$\boldsymbol{D}_6$	$\boldsymbol{D}_6$		0	0	0	equilibrium
$\boldsymbol{Z}_6$	E	M_3	$\xi(\theta)$	$\xi(\theta-k)$	$\xi(\theta-2k)$	$\xi(\theta)=-\xi(\theta+\pi), k\in\{+\mathrm{k}_3,-\mathrm{k}_3\}$
$\boldsymbol{Z}_3$	$\boldsymbol{Z}_3$		$\xi(\theta)$	$\xi(\theta)$	$\xi(\theta)$	
$\boldsymbol{Z}_3$	E		$\xi(\theta)$	$\xi(\theta-k)$	$\xi(\theta-2k)$	$k\in\{+\mathrm{k}_3,-\mathrm{k}_3\}$
$\boldsymbol{D}_2^{\rho}$	$\boldsymbol{Z}_2^{\rho}$	M_1	$\eta(\theta)$	$\xi(\theta)$	$\xi(\theta)$	$\xi(\theta)=-\xi(\theta+\pi), \eta(\theta)=-\eta(\theta+\pi)$
$\boldsymbol{D}_2^{\rho}$	$\boldsymbol{Z}_2^{\sigma}$	M_2	0	$\xi(\theta)$	$-\xi(\theta)$	$\xi(\theta)=-\xi(\theta+\pi)$
$\boldsymbol{Z}_2^{\rho}$	$\boldsymbol{Z}_2^{\rho}$		$\eta(\theta)$	$\xi(\theta)$	$\xi(\theta)$	
$\boldsymbol{Z}_2^{\rho}$	E		$\eta(\theta)$	$\xi(\theta)$	$\xi(\theta+\pi)$	$\eta(\theta)=\eta(\theta+\pi)$
$\boldsymbol{Z}_2^{\sigma}$	$\boldsymbol{Z}_2^{\sigma}$		0	$\xi(\theta)$	$-\xi(\theta)$	
$\boldsymbol{Z}_2^{\sigma}$	E		$\eta(\theta)$	$\xi(\theta)$	$-\xi(\theta+\pi)$	$\eta(\theta)=-\eta(\theta+\pi)$
$\boldsymbol{Z}_2$	E		$\boldsymbol{x}_{\mathrm{abc}}(\theta)=-\boldsymbol{x}_{\mathrm{abc}}(\theta+\pi)$			
E	E		$\xi(\theta)$	$\eta(\theta)$	$\zeta(\theta)$	asymmetric oscillation

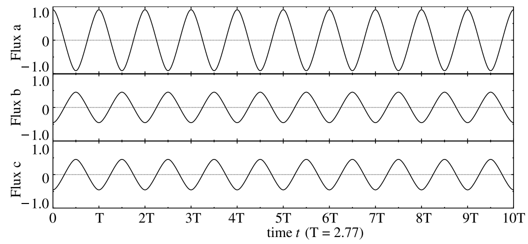

Fig. 8. Waveform of M_1. M_1 is type 1 and belongs to the subgroup $\boldsymbol{D}_2^{\rho}$.

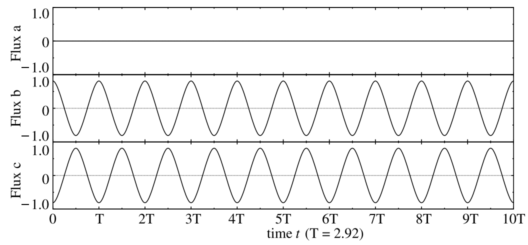

Fig. 9. Waveform of M_2. M_2 is type 2 and belongs to the subgroup $\boldsymbol{D}_2^{\rho}$.

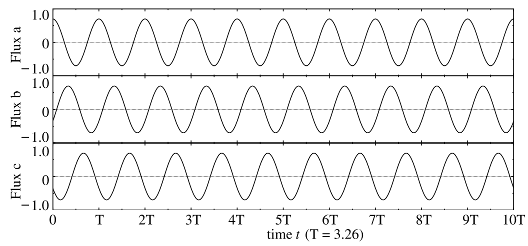

Fig. 10. Waveform of M_3. M_3 is type 3 and belongs to the subgroup $\boldsymbol{Z}_6$.

The symmetrical coordinates and the $0\alpha\beta$ coordinates used for power systems correspond to the symmetries $\boldsymbol{Z}_3$ and $\boldsymbol{D}_2^{\rho}$, respectively. The M_3 with $+\mathrm{k}_3$ and $-\mathrm{k}_3$ corresponds to positive-phase-sequence and negative-phase-sequence component in the symmetrical coordinate, respectively. The M_1 and M_2 correspond to α component and β component in the $0\alpha\beta$ coordinates, respectively. Thus, these results supports the well known coordinates in power systems [32].

5. Almost periodic oscillation

5.1 Definition

We extend the method of the classification for almost periodic oscillations. We define the almost periodic oscillation with normalized phase $\boldsymbol{\theta}$ by $\hat{\boldsymbol{x}}(\boldsymbol{\theta}):\mathbb{T}^2\mapsto\mathbb{R}^6$. Then, a subgroup H is defined by

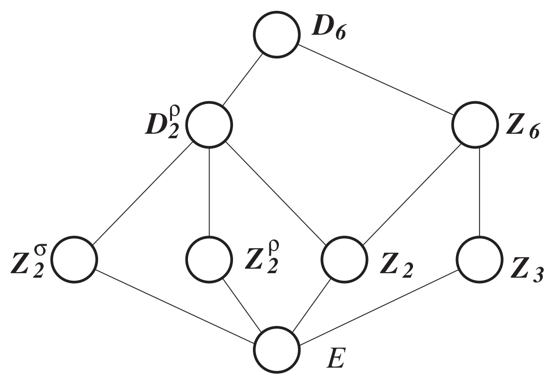

Fig. 11. Lattice of almost periodic oscillations.

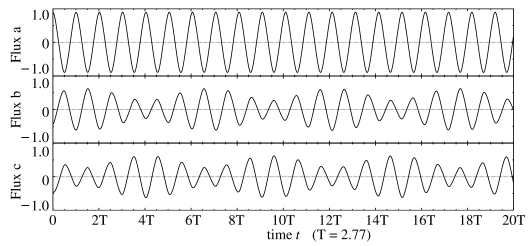

Fig. 12. Waveform of beat($\boldsymbol{D}_2^\rho$).

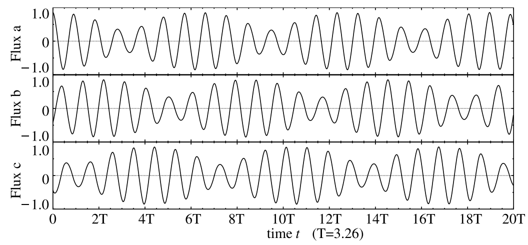

Fig. 13. Waveform of beat($\boldsymbol{Z}_6$).

$$H = \{\gamma \in \boldsymbol{D}_6 \mid \gamma\{\hat{\boldsymbol{x}}(\boldsymbol{\theta})\} = \{\hat{\boldsymbol{x}}(\boldsymbol{\theta})\}\} \tag{19}$$

for all the action $\gamma \in H$. The H-action preserves the trajectory of $\hat{\boldsymbol{x}}(\boldsymbol{\theta})$ and an action γ causes only a shift $\boldsymbol{k} \in \mathbb{T}^2$:

$$^\forall\boldsymbol{\theta} \in \mathbb{T}^2,\ \gamma\hat{\boldsymbol{x}}(\boldsymbol{\theta}) = \hat{\boldsymbol{x}}(\boldsymbol{\theta} - \boldsymbol{k}). \tag{20}$$

This relation defines a map $\boldsymbol{\Theta}(\gamma) : H \mapsto \mathbb{T}^2$ and the kernel of the map $\boldsymbol{\Theta}(\gamma)$ is defined by

$$K \triangleq \{\gamma \in H \mid \boldsymbol{\Theta}(\gamma) = \boldsymbol{o}\}\,. \tag{21}$$

The subgroup K defines the fixed-point subspace Eq. (18). The condition that $\boldsymbol{\Theta}$ is a group homomorphism is described by

$$H/K \cong \boldsymbol{Z}_{m_1} \times \boldsymbol{Z}_{m_2}, \tag{22}$$

where $m_1 \in \mathbb{Z}$ is a divisor of m_2 and $\mathbb{Z}$ denotes the set of integers. Additionally, Fix(K) is not less than 4. The conditions give the lattice of almost periodic oscillations with respect to the spatio-temporal symmetry H shown in Fig. 11 which is the same as Fig. 7. In this case, all the spatial symmetries K are E. Higher symmetric waveforms beat($\boldsymbol{D}_2^\rho$) and beat($\boldsymbol{Z}_6$) which belong to the subgroups $\boldsymbol{D}_2^\rho$ and $\boldsymbol{Z}_6$ respectively are shown in Figs. 12 and 13. The cyclic almost periodic oscillation beat($\boldsymbol{Z}_6$) in Fig. 13 corresponds to almost periodic type 3 oscillation shown in Fig. 4 and the almost periodic oscillation beat($\boldsymbol{D}_2^\rho$) in Fig. 12 is an almost periodic type 1 oscillation.

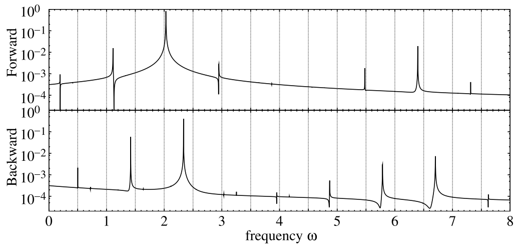

Fig. 14. The beat($\boldsymbol{Z}_6$) is decomposed into forward and backward components. The forward and backward components give the exclusive decomposition of the frequency components.

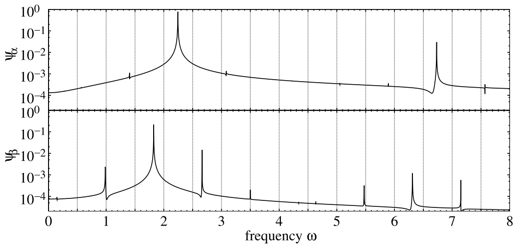

Fig. 15. The beat($\boldsymbol{D}_2^{\rho}$) is decomposed into α and β components. The α and β components give the exclusive decomposition of the frequency components.

5.2 Decomposition of almost periodic oscillation by symmetries

In order to characterize the almost periodic oscillations, we decompose the almost periodic oscillations based on the symmetries. First, we represent $\hat{\boldsymbol{x}}(\boldsymbol{\theta})$ by 2-dimensional Fourier series expansion:

$$\hat{\boldsymbol{x}}(\boldsymbol{\theta}) = \sum_{\boldsymbol{j} \in \mathbb{Z}^2} \boldsymbol{X}_{\boldsymbol{j}} \exp(\mathrm{j}\boldsymbol{j}^{\mathrm{T}}\boldsymbol{\theta}) + \text{c.c.}, \quad \boldsymbol{X}_{\boldsymbol{j}} \in \mathbb{C}^9, \tag{23}$$

where c.c. represents complex conjugate. Then, the 2-dimensional Fourier series expansion of Eq. (20) derives

$$\gamma \in H, \quad \gamma \boldsymbol{X}_{\boldsymbol{j}} = \exp(\mathrm{j}\boldsymbol{j}^{\mathrm{T}}\boldsymbol{k})\boldsymbol{X}_{\boldsymbol{j}}. \tag{24}$$

This equation shows that the vector $\boldsymbol{X}_{\boldsymbol{j}}$ is in the eigenspace of the action γ with respect to the eigenvalue $\lambda \triangleq \exp(\mathrm{j}\boldsymbol{j}^{\mathrm{T}}\boldsymbol{k})$. Using the eigenspaces and eigenvalues, we decompose the almost periodic oscillation $\hat{\boldsymbol{x}}(\boldsymbol{\theta})$.

For example, the flux $\hat{\boldsymbol{\psi}}_{\text{abc}} : \mathbb{T}^2 \mapsto \mathbb{R}^3$ with respect to the symmetry $\boldsymbol{Z}_6$ can be decomposed as

$$\begin{aligned}\hat{\boldsymbol{\psi}}_{\text{abc}}(\boldsymbol{\theta}) = & \sum_{\boldsymbol{j} \in \kappa_0 \cap \kappa_{\text{odd}}} \Psi_{0,j_1,j_2} \boldsymbol{w}'_0 \exp(\mathrm{i}(j_1\theta_1 + j_2\theta_2)\ ) \\ & + \sum_{\boldsymbol{j} \in \kappa_+ \cap \kappa_{\text{odd}}} \Psi_{+,j_1,j_2} \boldsymbol{w}'_+ \exp(\mathrm{i}(j_1\theta_1 + j_2\theta_2)\ ) \\ & + \sum_{\boldsymbol{j} \in \kappa_- \cap \kappa_{\text{odd}}} \Psi_{-,j_1,j_2} \boldsymbol{w}'_- \exp(\mathrm{i}(j_1\theta_1 + j_2\theta_2)\ ) + \text{c.c.},\end{aligned} \tag{25}$$

where

$$\begin{aligned}\kappa_0 &\triangleq \left\{\boldsymbol{j} \in \mathbb{Z}^2 \mid j_1 \mod 3 = 0\right\}, \\ \kappa_+ &\triangleq \left\{\boldsymbol{j} \in \mathbb{Z}^2 \mid j_1 \mod 3 = 1\right\}, \\ \kappa_- &\triangleq \left\{\boldsymbol{j} \in \mathbb{Z}^2 \mid j_1 \mod 3 = -1\right\}, \\ \kappa_{\text{odd}} &\triangleq \left\{\boldsymbol{j} \in \mathbb{Z}^2 \mid j_1 + j_2 \mod 2 = 1\right\}.\end{aligned} \tag{26}$$

We call the components in $\boldsymbol{w}'_0, \boldsymbol{w}'_+, \boldsymbol{w}'_-$ common mode (zero-phase sequence), forward mode (positive-phase sequence) and backward mode (negative-phase sequence), respectively. This decomposition

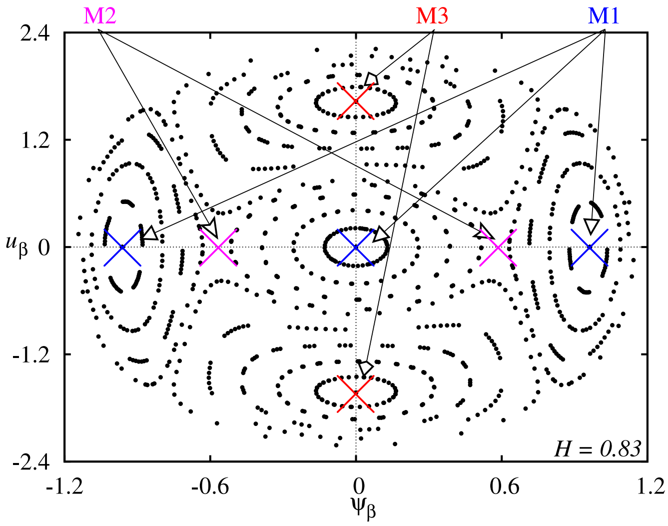

Fig. 16. Poincare map of the three LC ladder circuit. Periodic oscillations M_1, M_2, and M_3 exist and the almost periodic oscillations beat($\boldsymbol{D}_2^\rho$) and beat ($\boldsymbol{Z}_6$) exist around the M_1 and M_3, respectively. Almost all the phase space is covered by the regions of beat($\boldsymbol{D}_2^\rho$) and beat($\boldsymbol{Z}_6$).

(25) indicates that the spectra are also decomposed exclusively in the modes. Figure 14 shows the decomposition of cyclic almost periodic oscillation beat($\boldsymbol{Z}_6$). In this case, the components of common mode equal 0 and the coordinates enable the exclusive decomposition of the frequency components. Thus, we can understand that the almost periodic oscillation beat($\boldsymbol{Z}_6$) shown in Fig. 13 is the superposition of the forward and backward components.

In the same way, the almost periodic oscillation beat($\boldsymbol{D}_2^\rho$) also can be decomposed into α component Ψ_α and β component Ψ_β as shown in Fig. 15. We can understand that the almost periodic oscillation beat($\boldsymbol{D}_2^\rho$) shown in Fig. 12 is the superposition of the α and β components.

5.3 Structure of phase space

In order to clarify the structure of the phase space of Eq. (2), we calculate the Poincare map of a cross section

$$\Sigma \triangleq \{(\psi_\alpha, u_\alpha, \psi_\beta, u_\beta) | u_\alpha = 0, \psi_\alpha > 0\}, \tag{27}$$

where the suffixes α and β represent α and β coordinates [32].

Although the original phase space is 6-dimension, assuming that 0-phase components ψ_0 and u_0 are equal to 0 and fixing the total energy H, the Poincare map of all the phase space is represented in 2-dimensional plane. The Poincare map on ψ_α-ψ_β plane for the nonlinear function $i(\psi) = \psi + 3.8\psi^7$ and the total energy $H = 0.83$ is illustrated in Fig. 16. We can confirm that periodic oscillations M_1, M_2, and M_3 exist and the almost periodic oscillations beat($\boldsymbol{D}_2^\rho$) and beat($\boldsymbol{Z}_6$) exist around the M_1 and M_3, respectively. In this case, almost all the phase space is covered by the regions of almost periodic oscillation beat($\boldsymbol{D}_2^\rho$) and beat($\boldsymbol{Z}_6$) although the increase of the energy gives more complex oscillations [30]. Thus, we can confirm that the typical oscillations in the LC ladder circuit are M_1, M_2, M_3, beat($\boldsymbol{D}_2^\rho$), and beat($\boldsymbol{Z}_6$) and that these oscillations correspond to the typical oscillations type 1, 2, and 3 in the three-phase circuit.

6. Conclusion

Typical oscillation patterns in three-phase circuits are reviewed and are classified into the type 1, type 2 and type 3 based on the number of the related inductors. In order to give a reason for the typical patterns, we introduced the three LC ladder circuit which has a higher symmetry than the three-phase circuit and classified the periodic and almost periodic oscillations based only on the symmetries of the circuit. The lattice of the classified oscillations indicates that the M_1, M_2, and M_3 are typical patterns and the almost periodic oscillations are decomposed and characterized by each mode. Further, from the observation of the phase space, we confirmed that the typical patterns cover almost all the global phase space when the total energy is low. The discussions in this paper gives a reason for the typical patterns in the three-phase circuit by the symmetries.

Additionally, because the approach is based only on the symmetries of the circuit, there is a possibility that the classification can be applied to oscillations generated by other nonlinearities in symmetrical three-phase circuits. Even if the purpose of this paper is listing typical oscillation patterns only in a simple three-phase system and does not have the discussion about the stability of the patterns, the listed patterns could be applied in the analysis of power systems which contain wide varieties of nonlinear components. Further research of perturbed systems which give symmetry breaking also will be an interesting subject.

References

[1] Slow Transient Task Force of the IEEE Working Group on Modeling and Analysis of Systems Transients Using Digital Programs, M.R. Iravani, Chair, A.K.S. Chaudhary, W.J. Giesbrecht, I.E. Hassan, A.J.F. Keri, K.C. Lee, J.A. Martinez, A.S. Morched, B.A. Mork, M. Parniani, A. Sharshar, D. Shirmohammadi, R.A. Walling, and D.A. Woodford, "Modeling and analysis guidelines for slow transients – Part III: The study of ferroresonance," *IEEE Trans. PD*, vol. 15, no. 1, 2000.

[2] D.A.N. Jacobson, "Examples of ferroresonance in a high voltage power system," *IEEE PES General Meeting*, vol. 2, pp. 1206–1212, 2003.

[3] C. Kieny, "Application of the bifurcation theory in studying and understanding the global behavior of a ferroresonant electric power circuit," *IEEE Trans. PD*, vol. 6, no. 2, pp. 866–872, 1991.

[4] T.P. Tsao and C.C. Ning, "Analysis of ferroresonant overvoltages at Maanshan nuclear power station in Taiwan," *IEEE Trans. PD*, vol. 21, no. 2, pp. 1006–1012, 2006.

[5] J. Bethenod, "Sur le transformateur et resonance," *L'eclairae Electrique*, pp. 289–296, November 30, 1907.

[6] R. Rudenberg, *Transient Performance of Electric Power Systems*, NY: McGraw-Hill Book Company, New York, 1950, ch.48.

[7] C. Hayashi, *Nonlinear Oscillations in Physical Systems*, NY: McGraw-Hill Book Company, New York, 1964.

[8] Y. Ueda, *The Road to Chaos*, Aerial Press, Santa Cruz, CA, 1992.

[9] J.R. Marti and A.C. Soudack, "Ferroresonance in power systems: fundamental solutions," *Proc. IEE-C*, vol. 138, no. 4, pp. 321–329, 1991.

[10] A. Mork and D.L. Stuehm, "Application of nonlinear dynamics and chaos to ferroresonance in distribution systems," *IEEE Trans. PD*, vol. 9, no. 2, pp. 1009–1017, 1994.

[11] T. Yoshinaga and H. Kawakami, "Bifurcations and chaotic state in forced oscillatory circuits containing saturable inductors," In *T. Carroll and L. Pecora, Nonlinear Dynamics in Circuits*, pp. 89–118, World Scientific Publishing, 1995.

[12] T. Hisakado, T. Yamada, and K. Okumura, "Single-phase 1/3-subharmonic oscillations in three-phase circuit," *IEICE Trans. Fund.*, vol. 79-A, no. 9, pp. 1553–1561, 1996.

[13] F. Schilder, H.M. Osinga, and W. Vogt, "Continuation of quasi-periodic invariant tori," *SIAM J. Appl. Dyn. Syst.*, vol. 4, pp. 459–488, 2005.

[14] M. Goto, "Undamped electric oscillation and electric instability of transmission system," *Trans. IEEJ*, vol. 51, pp. 759–771, 1931.

[15] I.A. Wright, "Three-phase subharmonic oscillations in symmetrical power systems," *IEEE Trans PAS*, vol. 90, no. 3, pp. 1295–1304, 1971.

[16] D.R. Smith, S.R. Swanson, and J.D. Borst, "Overvoltages with remotely-switched cable-fed grounded wye-wye transformers," *IEEE Trans. PAS*, vol. 94, no. 5, pp. 1843–1853, 1975.

[17] K. Okumura and A. Kishima, "Nonlinear oscillations in three-phase circuit," *Trans. IEEJ*, vol. 96B, no. 12, pp. 599–606, 1976.

[18] N. Janssens, T. Van Craenenbroeck, D. Van Dommelen, F. Van De Meulebroeke, and L. Laborelec, "Direct calculation of the stability domains of three-phase ferroresonance in isolated neutral networks with grounded-neutral voltage transformers," *IEEE Trans. PD*, vol. 11, no. 3, pp. 1546–1553, 1996.

[19] M. Golubitsky, I. Stewart, and D.G. Schaeffer, *Singularities and Groups in Bifurcation Theory II*, Applied Mathematics Science, 69, Springer Verlag, New York, 1988.

[20] M. Golubitsky and I. Stewart, *The Symmetry Perspective*, Chapter 3, Birkhauser Verlag, 2003.

[21] T. Van Craenenbroeck, W. Michiels, D. Van Dommelen, and K. Lust, "Bifurcation analysis of three-phase ferroresonant oscillations in ungrounded power systems," *IEEE Trans. PD*, vol. 14, no. 2, pp. 531–536, 1999.

[22] T. Hisakado and K. Okumura, "Bifurcation phenomena of 1/2-subharmonic oscillations in three-phase circuit," *IEICE Trans. Fundamentals*, vol. E82-A, no. 9, pp. 1919–1925, 1999.

[23] T. Hisakado and K. Okumura, "Two-phase 1/3-subharmonic oscillations in three-phase circuit," *IEICE Trans. Fundamentals*, vol. J80-A, no. 2, pp. 355–362, 1997.

[24] T. Hisakado and K. Okumura, "Bifurcation phenomena of harmonic oscillations in three-phase Circuit," *IEICE Trans. Fundamentals*, vol. E80-A, no. 6, pp. 1127–1134, 1997.

[25] T. Hisakado and K. Okumura, "Cnoidal wave in symmetric three-phase circuit," *IEE Proc.-Circuits Devices Syst.*, vol. 152, no. 1, pp. 49–53, 2005.

[26] T. Hisakado and S. Ukai, "Appearance of intrinsic localized mode in three-phase circuit," *Proc. NDES2007*, pp. 110–113, 2007.

[27] R.M. Rosenberg, "Normal modes of nonlinear dual-mode systems," *Journal of Applied Mechanics*, vol. 27, pp. 263–268, 1960.

[28] G. Kerschen, M. Peeters, J.C. Golinval, and A.F. Vakakis, "Nonlinear normal modes, Part I: A useful framework for the structural dynamicist," *Mechanical Systems and Signal Processing*, vol. 23, pp. 170–194, 2009.

[29] P. Poggi and S. Ruffo, "Exact solutions in the FPU oscillator chain," *Physica D*, vol. 103, pp. 251–272, 1997.

[30] G.P. Berman and F.M. Izrailev, "The Fermi-Pasta-Ulam problem: Fifty years of progress," *Chaos*, vol. 15, 015104, 2005.

[31] B.F. Feng, "An integrable three particle system related to intrinsic localized modes in Fermi-Pasta-Ulam-chain-β," *J. Phys. Soc. Jpn.*, vol. 75, 2006.

[32] Y. Hase, *Handbook of Power System Engineering*, John Wiley & Sons, 2007.